



Deposited via The University of Sheffield.

White Rose Research Online URL for this paper:

<https://eprints.whiterose.ac.uk/id/eprint/108429/>

Version: Accepted Version

Proceedings Paper:

Fox, C.W. and Prescott, T.J. (2011) Mapping with Sparse Local Sensors and Strong Hierarchical Priors. In: Groß, R., Alboul, L., Melhuish, C., Witkowski, M., Prescott, T.J. and Penders, J., (eds.) Towards Autonomous Robotic Systems. TAROS 2011, August 31 - September 2, 2011, Sheffield, UK. Lecture Notes in Computer Science, 6856. Springer, Berlin, Heidelberg, pp. 183-194. ISBN: 978-3-642-23231-2. ISSN: 0302-9743.

https://doi.org/10.1007/978-3-642-23232-9_17

Reuse

Items deposited in White Rose Research Online are protected by copyright, with all rights reserved unless indicated otherwise. They may be downloaded and/or printed for private study, or other acts as permitted by national copyright laws. The publisher or other rights holders may allow further reproduction and re-use of the full text version. This is indicated by the licence information on the White Rose Research Online record for the item.

Takedown

If you consider content in White Rose Research Online to be in breach of UK law, please notify us by emailing eprints@whiterose.ac.uk including the URL of the record and the reason for the withdrawal request.

Mapping with sparse local sensors and strong hierarchical priors

Charles Fox

Tony Prescott

Abstract—The paradigm case for robotic mapping, as in Simultaneous Localisation and Mapping problems, considers a mobile robot with noisy odometry and laser scanners. Laser scanners provide large amounts of sensory information, and have effectively unlimited range in indoor environments. Such large quantities of input information allow the use of relatively weak priors. In contrast, the present study considers the mapping problem in environments where only sparse, local sensory information is available. To compensate for the lack of likelihood evidence, we make use of strong hierarchical object priors. Hierarchical models were popular in classical blackboard systems but here are applied in a Bayesian setting and novel deployed as a mapping algorithm. We give proof of concept results, intended to demonstrate the algorithm’s applicability as a part of a tactile SLAM module for the whiskered ScratchBot mobile robot platform.

I. INTRODUCTION

The paradigm case for robotic mapping, as in Simultaneous Localisation and Mapping (SLAM) problems [1], considers a mobile robot with noisy odometry and SICK laser scanners. Laser scanners provide large amounts of sensory information, and have effectively unlimited range in indoor environments. Such large quantities of input information allow the use of relatively weak priors, such as independent grid cell occupancy or flat priors over the belief of small feature sets [1].

In contrast, the present study considers the mapping problem in environments where only sparse, local sensory information is available. For example, a fire-fighting robot building up a map in a smoke-filled house cannot rely on laser scanners functioning at all times, and could instead operate by feeling its way around with touch sensors. Proof that this type of navigation is possible is found in biology: electric fish make use of highly localised electric field sensors [2] and rats navigate through dark underground tunnels using their whiskers [3], [4], both having ranges of a few centimetres. In robotics, touch sensors are relatively cheap in both material and computational processing terms, and their use has previously been considered to enhance navigation in cheap household robots [5], [6]. (Related work on research robot platforms includes [7], [8], [9], [10], [11]).

As an example of this type of mapping, we consider the case of a mobile robot having six whiskers, able to report the (noisy) locations and orientations of contacts with surfaces. Such mechanical sensors and computational classifiers have previously been demonstrated in [5], [6], [12], and are able

Charles Fox and Tony Prescott are with the Active Touch Laboratory at Sheffield (ATL@S), University of Sheffield, S10 2TN, UK. Email: charles.fox@sheffield.ac.uk This work was supported by EU FP7 Biomimetic Architectures for Active Touch (BIOTACT), ICT- 215910.

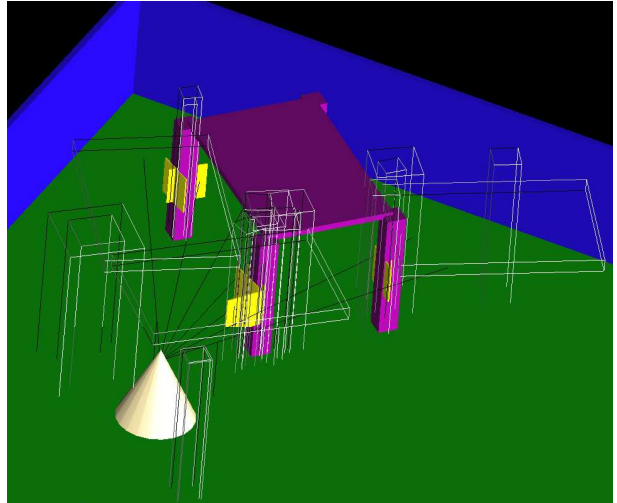


Fig. 1. Simulation screen-shot at high temperature. Many hypothesised (wire-frame) tables and legs are on the blackboard, primed by the shapelets (yellow rectangles) contacted by the robot (cone)’s whisker sensors, in an arena containing a physical table (pink).

to report locations, orientations and textures of contact points (note that textures are especially difficult to report using other sensor modalities). The present mapping algorithm is intended to form part of a future SLAM navigation module for the whiskered ScratchBot hardware platform [13], but here we give a proof of concept mapping-only algorithm in a simulated and simplified microworld. It is the first work to begin fusing whisker contact reports to perform mapping.

To compensate for the sparseness of the sensory information available from short-range touch sensors, we make use of strong, hierarchical priors about objects in the world. Hierarchical object recognition models were popular in classical, symbolic AI in the guise of blackboard systems [14], [15], [16] but have recently been recast in terms of dynamically constructed Bayesian networks [17], [18], [19], [20]. Here we provide a novel application of Bayesian blackboards to the robotic mapping problem.

Object based mapping models have recently appeared [21], [22], [23], [24] which use laser sensors to recognise and learn complex spatial models. However in the sparse local sensor case, this level of detail is unavailable, and only a few contact points may be present. Thus we go beyond the use of individual movable objects, to use strong hierarchical model priors. For example, on recognising a table leg, we may then infer the probable presence the rest of the table, including other leg objects, and edges and corners making up

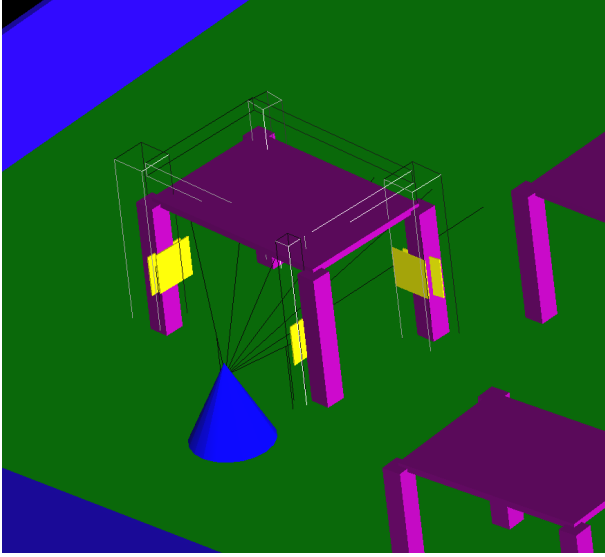


Fig. 2. Simulation screen-shot at low temperature. A single table hypothesis remains.

these legs, without ever sensing them directly. To construct hierarchical objects, we use hypothesis priming and pruning heuristics as in blackboard systems. However, following [17], we treat such heuristics as approximations to inference in a dynamically-constructed, Monte Carlo Markov Chain (MCMC) sampling Bayesian network, endowing them with probabilistic semantics.

II. METHODS

A. Minidomain task

Consider the task of building a map of an arena populated by four-legged table-like objects as in figs. 1 and 2. (Such objects could include chairs and desks for example). A mobile whiskered agent moves along a predetermined trajectory of location-angle poses, (x_t, y_t, θ_t) , around the arena, over discrete time steps t . At each time step, its six whiskers ($w \in 0 : 5$) report the radial distance r to, and surface normal ϕ and texture τ of, any contacts made with the tables,

$$\hat{r}_t^w = r_t^w + \varepsilon_r, \quad (1)$$

$$\hat{\phi}_t^w = \phi_t^w + \varepsilon_\phi, \quad (2)$$

$$\hat{\tau}_t^w = \tau_t^w + \varepsilon_\tau, \quad (3)$$

where ε are i.i.d. Gaussian noises having zero mean and standard deviations $\sigma_r^w, \sigma_\phi^w, \sigma_\tau^w$ respectively.

B. Static structures: generative models

Tables, T , are parametrised by tuples, $T(x_T, y_T, \theta_T, w_T^L, \tau_T)$, where x, y is the location, θ is the pose angle, w^L is the width of their (square) legs, and $\tau \in (0, 1)$ is a texture parameter describing roughness or smoothness of the material. A generative model of tables is used. We assume a flat prior probability density generating tables in the world,

$$p(x, y, \theta, w_L, \tau) = c_T, \quad (4)$$

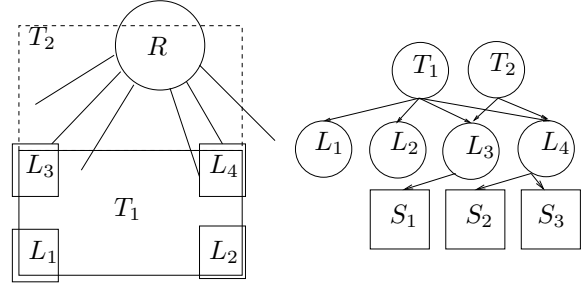


Fig. 3. Hierarchical object recognition. *Left*: Robot R (circle) with six whiskers (lines) makes tactile contact with legs L_j (squares) of a hypothesised table T_1 (rectangle). The two contact points ('shapelets') on the right are sufficient to infer the location of the corner of leg L_4 . Coupled with prior knowledge about the shape and size of tables, and the third shapelet, this can be used to infer that there is a table either in the ground truth location or in a second configuration T_2 (dashed rectangle). *Right*: Bayesian network constructed to represent the same scenario. Square nodes are the shapelet observations.

where c_T is a constant. (c_T is *not* required to normalise the distribution, but is chosen so that $\int_A p(x, y, \theta, w^L, \tau) \leq 1$ over the arena A).

If a table T exists, its presence causes (in Pearl's sense [25]) the presence of four leg objects $L(x_L, y_L, \theta_L, w_L^x, w_L^y, \tau_L, T)$, where w^x, w^y are the width and breadth of the table leg; x, y, θ are its location and rotation, and τ is its texture, with probability density

$$p(L(x_L, y_L, \theta_L, w_L^x, w_L^y, \tau_L, T) | T(x_T, y_T, \theta_T, w_T^L, \tau_T)) = \alpha_L \exp -\Delta_{TL}, \quad (5)$$

where α is a generally *non-normalising* constant describing the overall probability of *some* legs being generated, and the distance measure is

$$\Delta_{TL} = \min_i \left(\frac{(x_T^i - x_L)^2 + (y_T^i - y_L)^2}{\sigma_r^2} \right) + \left(\frac{\theta_T - \theta_L}{\sigma_\theta} \right)^2 + \left(\frac{w_T^L - w_L^x}{\sigma_w} \right)^2 + \left(\frac{w_T - w_L^y}{\sigma_w} \right)^2 + \left(\frac{\tau_T - \tau_L}{\sigma_\tau} \right)^2, \quad (6)$$

where i ranges over the four legs of the table, and (x_T^i, y_T^i) are the coordinates of its corners. The inclusion of T in the parametrisation of L denotes that L is the hypothesis that the leg was caused only by table T rather than any other tables or causes.

If contacted by the robot's whiskers, (and assuming perfect robot localisation in the present study only) the leg objects cause *shapelet* reports, $S(x_S, y_S, \theta_S, \tau_S)$. These report the position, surface normal, and texture of the contact, and again are subject to Gaussian noise. Such reports are currently available on the ScratchBot hardware platform, [13], [5], [6] but are simulated in the present study by

$$p(S(x_S, y_S, \theta_S, \tau_S) | L(x_L, y_L, \theta_L, w_L^x, w_L^y, \tau_L)) = \alpha_S \exp -\Delta_{LS}$$

where

$$\Delta_{LS} = \min_r \left(\frac{r}{\sigma_r} \right)^2 + \left(\frac{\theta_L - \theta_S}{\sigma_\theta} \right)^2 + \left(\frac{\tau_L - \tau_S}{\sigma_\tau} \right)^2, \quad (7)$$

and r is the shortest radial distance from any point on the perimeter of the leg to (x_S, y_S) , computed by basic geometry.

We also allow legs and shapelets to be caused by chance, rather than by generative parents. That is, we allow a (small) prior that a single leg exists by itself, or that a shapelet exists with no macroscopic parent (these are required during construction on the blackboard). Such causation is modelled with the flat ‘null’ priors,

$$p(L(x_L, y_L, \theta_L, w_L^x, w_L^y, \tau_L, \emptyset | \emptyset) = c_L, \quad (8)$$

$$p(S(x_S, y_S, \theta_S, \tau_S) | \emptyset) = c_S, \quad (9)$$

with constants such that the marginalised densities,

$$p(S(x_L, y_L, \theta_L) < p(L(x_L, y_L, \theta_L) < p(T(x_L, y_L, \theta_L), \quad (10)$$

i.e. larger objects are more probable to exist without high-level causes than smaller objects are.

Shapelets may be caused by multiple leg hypotheses, and by the null prior (eqn. 9). For example if there are two legs very close together then the density for shapelets in the area increases. We assume that multiple causal sources combine using noisy-OR semantics,

$$P(x_i | pa(x_i)) = 1 - \prod_{x_j \in pa(x_i)} (1 - P(x_i | x_j)). \quad (11)$$

As we use probability *density* functions we require the continuous version of noisy-OR, proved in the Appendix:

$$p(x_i | pa(x_i)) = \sum_{x_j \in pa(x_i)} p(x_i | x_j). \quad (12)$$

Similarly, legs may be caused both by their (single) specified parent (i.e. the T parameter in eqn. 5) and the null prior (eqn. 8), so use a similar combination rule to fuse these two causes. Tables can only be caused by the null prior (eqn. 4).

Taken together, the equations in this section define a Bayesian network for any given collection of tables, legs and shapelets as shown in fig. 3. However, in addition to the previous causal probabilities, we require probability factors to model the following constraints: (a) tables always have four legs; (b) each table leg is at a different corner of the table (we should not see two legs attached to the same corner); (c) two objects of the same type (table or leg) cannot overlap in physical space. Standard Bayesian networks cannot model such relations, as they are limited to joint distributions of the form

$$P(\{x_i\}_i) = \prod_i P(x_i | pa(x_i)), \quad (13)$$

where $pa(x_i)$ denotes the set of parents of node x_i . To model these additional constraints, we extend the Bayesian network to the factor graph,

$$P(\{x_i\}_i) = \frac{1}{Z} \left(\prod_i P(x_i | pa(x_i)) \right) \times \left(\prod_{ij} \phi_c(x_i, x_j) \phi_b(x_i, x_j) \right) \left(\prod_i \phi_a(x_i) \right), \quad (14)$$

Algorithm 1 Blackboard-inspired approximate Metropolis-hasting proposals generation.

```

for each time step  $t$  do
  update shapelet set  $S$ 
  for each annealing temperature  $\beta$  do
    for each shapelet  $S_i \in S$  do
      propose and test parent  $H_i$  from  $Q(pa(S_i))$ 
      if accepted, add  $H_i$  to hypothesis set  $B$ 
    end for
    for each hypothesis  $H_i \in B$  do
       $r \leftarrow rand(0, 1)$ 
      if  $r < r_1$  then
        propose death of  $H_i$ 
        if accepted, remove  $H_i$  from  $B$ 
      else
        if  $r < r_2$  then
          propose parent change for  $H_i$ 
          if accepted, replace  $H_i$ 's parent parameter
        else
          if  $r < r_2$  then
            propose child  $h_j$  from  $Q(ch(H_i) | H_i)$ 
            if accepted, add  $H_j$  to hypothesis set  $B$ 
          else
            propose parent  $h_j$  from  $Q(pa(H_i) | H_i)$ 
            if accepted, add  $H_j$  to hypothesis set  $B$ 
          end if
        end if
      end if
    end for
  end for
  prune all hypotheses not linked to any shapelet directly
  or via a common ancestor.
end for

```

where Z is a normalising constant, and ϕ_a, ϕ_b, ϕ_c are unnormalised penalty factors corresponding to the three new constraints. We use

$$\phi_a(x_i) = \epsilon^m, \quad (15)$$

where m is the number of missing legs iff x_i is a table, and $m = 0$ otherwise. Similarly,

$$\phi_c(x_i, x_j) = \epsilon^v, \quad (16)$$

where v is a Boolean (0,1) value, true if hypotheses x_i and x_j are of the same type and overlap in physical space. Finally,

$$\phi_b(x_i, x_j) = \epsilon^r, \quad (17)$$

where r is a Boolean, true if hypotheses x_i and x_j are legs and share the same parent (recalling the parametrisation of leg hypotheses on particular tables).

C. Inference

For a given set of shapelet observations and a set of candidate hierarchical legs and tables, we may thus construct

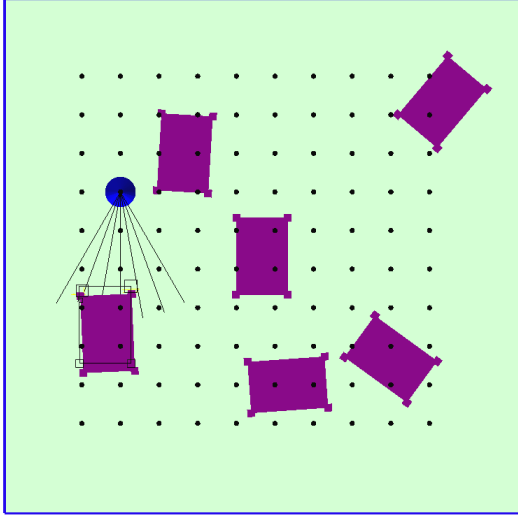


Fig. 4. Overhead view showing ground truth table configuration, and locations (black dots) of the discrete poses occupied by the robot. There are four angle poses at each location, facing in compass directions.

a factor graph. (We later describe how such a set of candidates is obtained automatically). Inference becomes highly complicated if the agent has an infinite memory for shapelets, so in the present study we use a working memory of the seven most recent shapelets, and discard all others. At each t , new shapelets are read from the sensors, and inference is performed with the aim of obtaining the Maximum A Posterior (MAP) interpretation of their causes, before the next time step begins,

$$\text{MAP} = \arg_{\{T_j\}} \max P(\{T_j\}_j | \{S_k\}_k). \quad (18)$$

Thus we currently treat each time step as an independent inference problem. Limiting inference to the most recent shapelets also has the effect of working within a local ‘fovea’ of attention: if no recent shapelets are from distant areas, then only hypotheses around the agent’s location will be considered.

There is some subtlety in defining the meaning of MAP states in continuous parameter spaces. In the present study, we assume that discrete hypotheses $H_i(x, y, \theta, \Theta)$ (where $H \in \{S, L, T\}$) represent small but non-infinitesimal collections of possible (x, y, θ) poses, with probability

$$\begin{aligned} P(H((x - \delta, x + \delta), (y - \delta, y + \delta), (\theta - \delta, \theta + \delta), \Theta)) \\ = (2\delta)^3 p(H(x, y, \theta, \Theta)), \end{aligned} \quad (19)$$

where δ is a small but nonzero constant, Θ are the remaining parameters, and p is the density.

We use the annealed [26] approximate Metropolis-Hastings sampler of algorithm 1 to perform inference. Unlike standard inference problems, object-based mapping is a form of scene analysis task, i.e. the number of objects in the world – and therefore the number and type of nodes in the network – is unknown in advance. Algorithm 1 uses blackboard-like

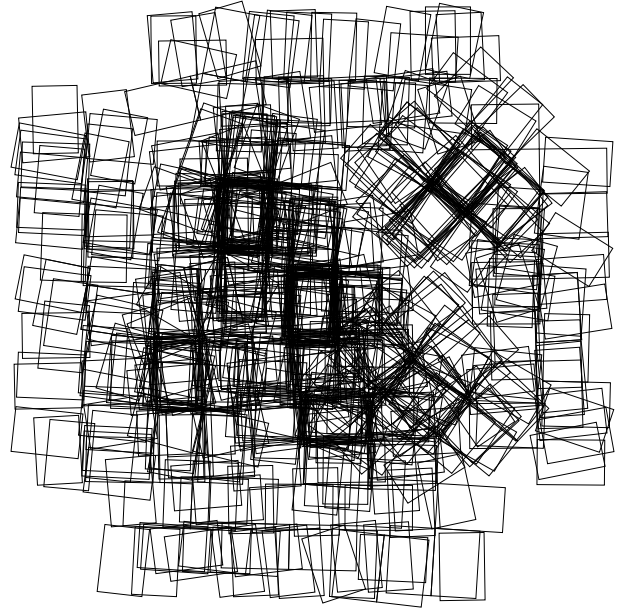


Fig. 5. Montage showing the collection of inferred tables from each independent robot pose.

priming and pruning heuristics integrated with the sampling, to control the size of the network.

Details of the algorithm are as follows. Each hypothesis in the current ‘blackboard’ set B maintains (amongst other parameters), pose parameters x, y, θ and a current parent. (The purpose of the explicit parent parameter is to model constraint (b)). The current parent may be another hypothesis, or may be null. Importantly, hypotheses that are not true are never stored in B . The set B acts as a factor graph as detailed in the previous section, and may be thought of as the contents of a blackboard [14].

To obtain unbiased samples from the true joint distribution, Metropolis-Hastings sampling requires detailed technical conditions to be met, which are complicated by the jumps between factor graphs of different structures and sizes. Reversible jump methods [27] provide a rigorous theoretical basis from which to define acceptance probabilities based on reweighting proposals. Future work should incorporate such theory, for now we heuristically choose the Q distributions and r_i thresholds; and use the annealed original P distribution from the factor graph as a simple Gibbs [26] acceptance probability,

$$P(\text{accept}H_i) \leftarrow P^\beta(H_i | mb(H_i)), \quad (20)$$

where $mb(H_i)$ is the Markov blanket of H_i , β is inverse temperature, and the arrow describes drawing a sample from the distribution. The Markov blanket conditional is

$$\begin{aligned} P(H_i | mb(H_i)) &= P(H_i | pa, ch, riv) \\ &= \frac{1}{Z} \frac{\phi_a(H_i) \phi_b(H_i, rivs) \phi_c(H_i, rivs) P(H_i | pa) P(ch | H_i)}{P(ch | (H_i)) P(H_i | pa) + P(ch | \neg H_i) P(\neg H_i | pa)} \\ &= \frac{1}{Z} \frac{\phi_a(H_i) \phi_b(H_i, rivs) \phi_c(H_i, rivs) p(H_i | pa) p(ch | H_i)}{\delta^3 (p(ch | H_i) p(H_i | pa) + p(ch | \neg H_i) p(\neg H_i | pa))}, \end{aligned}$$

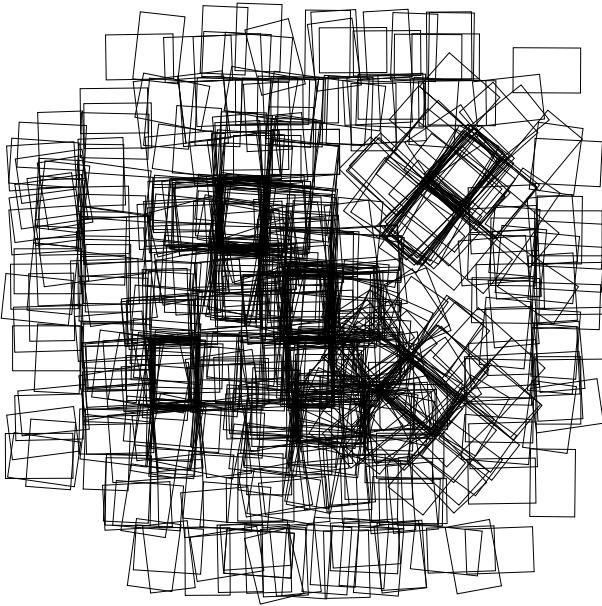


Fig. 6. Montage showing the collection of inferred tables from each independent robot pose, for ideal, noiseless sensors.

where $pa = pa(H_i)$, $ch = ch(H_i)$, $rivs = rivs(H_i)$; δ is the constant of eqn. 19; and ϕ_a includes missing children of H_i and also the missing child penalty for each parent of H_i which would have a missing child in the case where H_i is false. The update allows computation to proceed using density functions rather than probabilities, but includes δ .

When proposing a change in parent parameter for H_i , it is necessary to locate all potential parents $pa(H_i)$ to choose from. A threshold radius in pose space is used, which limits this set to candidates which are close enough to have non-negligible generating probabilities $P(H_i|H_j)$, $H_j \in pa(H_i)$. For computational efficiency it is useful to implement a spatial hash-table to look up nearby hypotheses. This hash-table may also be reused to look up overlapping hypotheses in the computation of ϕ_c .

III. RESULTS

We have implemented a simple simulation of a whiskered robot in a world populated by six four-legged, table-like objects, in a simple mapping task. The simulation is coded in C++ using the ODE physics engine (www.ode.org) for collision detection. Source code is available on request. The agent follows a fixed sequences of poses around the world and runs algorithm 1 once at each pose. There are $10 \times 10 \times 4$ poses, from 10 discrete x and y positions and four compass θ angles, as shown in fig. 4. To further simplify the present simulation, tables are all of a fixed size and have identical leg width and texture parameters.

TODO: say what noise levels and priors used

Steps in the inference are illustrated in the supplemental video material. The MAP hypothesis sets from all poses are collated and plotted onto a map of the arena in fig. 5. Comparing against the ground truth in fig. 4, the collated plot shows that table hypotheses are usually found in the correct

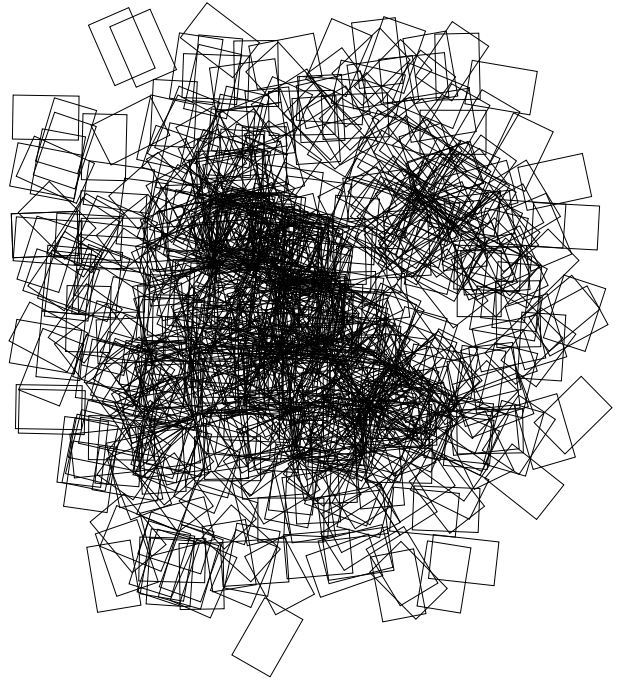


Fig. 7. Montage showing the collection of inferred tables from each independent robot pose, for very noisy ($\sigma_r = 0.5$, $\sigma_\theta = \pi/8$) sensors.

locations, corresponding to the real tables. The average number of whiskers contacting tables at each pose having at least one table contact is 4.2 ± 1.7 . As we would expect from such a sparse amount of data, there are thus many incorrect hypotheses found in MAPs of the form shown in fig. 3. These are created from poses which do not provide enough information about the tables to resolve ambiguities, for example when the robot is close enough to touch two legs but no third leg as in fig. 3. Also of interest in the results are the many table hypotheses perceived around the edge of the arena. These are due to the agent observing shapelets from contact with the walls around the arena. The system does not (yet) have perceptual models of walls, so the best available explanations for such shapelets are those which postulate tables with legs at these shapelet locations. (This is a form of perceptual relativism: lacking a WALL concept, the system explains the data using its best available TABLE theories.) Similar plots for noiseless and highly noisy sensor cases are shown in figs. 6 and 7 for comparison. In both cases, the approximate locations of inferred tables are similar, though the accuracy of inferred table poses depends on the noise.

IV. DISCUSSION

We have presented a proof-of-concept simulation of a novel framework for hierarchical object-based mapping from sparse local sensors, such as whiskers and other types of touch; but also applicable to sensors such as low-power or covert short range scanners; or local field-based sensors as used by electric fish.

Many simplifications were made in this proof-of-concept, which future versions of the system should relax. The results

presented here are simply the collation of many independent inferences made from the different poses in the sequence, and no information is shared between poses. Storing longer-term memories of shapelets and fusing them into the inferences would obviously allow a more refined map of the arena to be constructed: at present each table shown in the results has been inferred from typically three or four shapelets only. The present system makes no use of negative evidence, i.e. the observed absence of shapelets on non-contacting whiskers: this could be used to remove some of the ambiguous percepts. The heuristic threshold constants in the proposal distribution should be replaced with Reversible Jump MCMC reweightings to remove bias in the sampling distribution (although in practice the heuristic thresholds can work well, as ultimately only the annealed MAP is sought, rather than an approximation to the whole distribution).

Importantly, the proof-of-concept simulation operates in a world having only one size and texture of table (though tables may have different leg sizes). Enlarging the parameter space to range over tables sizes and textures will allow inference of more realistic four-legged objects such as different kinds of chairs and desks. Other types of objects could also be introduced, such as walls, kitchen units and radiators. The Bayesian blackboard architecture is able to automatically select between rival object models, treating them as rival hypotheses [17]. However, as the number of models and parameters grows, sampling of course becomes less efficient. For example, it becomes less probable that a perfectly-fitting table will ever be proposed. (Even though once proposed, it will tend to remain accepted for having such a good fit.) We plan to investigate the use of ‘smart proposals’ which are classical heuristic object detectors (e.g. Hough transforms to find edges and corners) but re-purposed as Metropolis-Hastings proposals in the Bayesian Blackboard. When combined with RJ-MCMC acceptance probabilities, this gives a way to speed up the proposals but retain the probabilistic semantics.

We next hope to extend our implementation to recognise several types of object of varying size, and move from simulation to the ScratchBot platform [13], which is currently able to report shapelets of the form used in simulation. ScratchBot includes noisy odometry, so will require our mapping system to function as part of a SLAM system. New forms of loop-closure in SLAM may become possible by recognising different parts of the same hierarchical object.

REFERENCES

[1] S. Thrun, W. Burgard, and D. Fox, *Probabilistic Robotics*. MIT Press, 2006.
 [2] W. Heiligenberg, *Neural nets in electric fish*. MIT Press, 1991.
 [3] G. Carvell and D. Simons, “Biometric analyses of vibrissal tactile discrimination in the rat,” *J. Neurosci.*, vol. 10, no. 8, p. 2638, 1990.
 [4] A. Ahl, “The role of vibrissae in behavior: a status review,” *Veterinary Research Communications*, vol. 10, no. 1, pp. 245–268, 1986.
 [5] N. Lepora, M. Evans, C. Fox, M. Diamond, K. Gurney, and T. Prescott, “Naive Bayes texture classification applied to whisker data from a moving robot,” *Proc. IEEE World Congress on Comp. Int. WCCI2010*.
 [6] M. Evans, C. Fox, M. Pearson, and T. Prescott, “Spectral Template Based Classification of Robotic Whisker Sensor Signals in a Floor Texture Discrimination Task,” *Proceedings TAROS2009*, pp. 19–24.

[7] A. Seth, J. McKinstry, G. Edelman, and J. Krichmar, “Texture discrimination by an autonomous mobile brain-based device with whiskers,” in *Proc. IEEE Int. Conf. Robot. Autom. ICRA2004*, pp. 4925–4930.
 [8] A. Schultz, J. Solomon, M. Peshkin, and M. Hartmann, “Multifunctional whisker arrays for distance detection, terrain mapping, and object feature extraction,” *Proc. ICRA2005*, pp. 2588–2593.
 [9] D. Kim and R. Moller, “Biomimetic whiskers for shape recognition,” *Robotics and Autonomous Systems*, vol. 55, no. 3, pp. 229–243, 2007.
 [10] M. Kaneko, N. Kanayama, and T. Tsuji, “Active antenna for contact sensing,” *IEEE Transactions on robotics and automation*, vol. 14, no. 2, pp. 278–291, 1998.
 [11] M. Fend, “Whisker-based texture discrimination on a mobile robot,” *Advances in Artificial Life*, pp. 302–311, 2005.
 [12] M. Evans, C. Fox, and T. Prescott, “Tactile discrimination using template classifiers: Towards a model of feature extraction in mammalian vibrissal systems,” *From Animals to Animats SAB2010*.
 [13] M. J. Pearson, B. Mitchinson, J. Welsby, A. G. Pipe, and T. J. Prescott, “Scratchbot: Active tactile sensing in a whiskered mobile robot,” *From Animals to Animats SAB2010*.
 [14] L. Erman, F. Hayes-Roth, V. Lesser, and R. Reddy, “The Hearsay-II speech understanding system,” *ACM Computing Surveys*, vol. 12, no. 2, June 1980.
 [15] M. Mitchell, *Analogy-Making as Perception*. MIT, 1993.
 [16] T. Binford and T. Levitt, “Evidential reasoning for object recognition,” *IEEE Transactions on Pattern Analysis and Machine Intelligence*, 2003.
 [17] C. Fox, “ThomCat: A Bayesian blackboard model of hierarchical temporal perception,” in *Proceedings of the 21st International Florida Artificial Intelligence Research Society Conference*, 2008.
 [18] B. Milch, “Probabilistic models with unknown objects,” Ph.D. dissertation, UC Berkeley, 2006.
 [19] K. B. Laskey and P. C. da Costa, “Of starships and klingons: Bayesian inference for the 23rd century,” in *Proc. UAI*, 2005.
 [20] C. Sutton, B. Burns, C. Morrison, and P. R. Cohen, “Guided incremental construction of belief networks,” in *Proceedings of the Fifth International Symposium on Intelligent Data Analysis*, 2003.
 [21] C.-C. Wang, C. Thorpe, S. Thrun, M. Herbert, and H. Durrant-Whyte, “Simultaneous localization, mapping and moving object tracking,” *International Journal of Robotics Research*, vol. 26, p. 889, 2007.
 [22] G. Gallagher, S. S. Srinivasa, J. A. Bagnell, and D. Ferguson., “Gatmo: A generalized approach to tracking movable objects,” in *ICRA*, 2009.
 [23] S. Srinivasa, D. Ferguson, C. Helfrich, D. Berenson, A. C. Romea, R. Diankov, G. Gallagher, G. Hollinger, J. Kuffner, and J. M. Vandeweghe, “Herb: a home exploring robotic butler,” *Autonomous Robots*, vol. 28, no. 1, pp. 5–20, January 2010.
 [24] A. Petrovskaya, O. Khatib, S. Thrun, and A. Y. Ng, “Touch based perception for object manipulation,” in *ICRA*, 2007.
 [25] J. Pearl, *Causality*. Cambridge University Press, 2000.
 [26] E. Aarts and J. Korst, *Simulated Annealing and Boltzmann Machines*. Wiley, 1988.
 [27] P. Green, “Reversible jump markov chain monte carlo computation,” *Biometrika*, vol. 82, no. 4, pp. 711–732, 1995.

APPENDIX: NOISY-OR DENSITY COMBINATION

Let Y_i range over node $pa(X)$ in a continuous-valued Bayesian network with noisy-OR parent combinations,

$$P(X|\{Y_i\}_i) = 1 - \prod_i (1 - P_i). \quad (21)$$

Consider the probability of a small range of hypotheses,

$$\delta^3 p(X|\{Y_i\}_i) = 1 - \prod_i (1 - \delta^3 p_i), \quad (22)$$

where p are probability densities and P are probabilities. Expansion terms with powers of δ that are > 3 vanish, so

$$\delta^3 p(X|\{Y_i\}_i) = \delta^3 \sum p_i. \quad (23)$$

The δ^3 terms cancel to yield

$$p(X|\{Y_i\}_i) = \sum p_i. \quad (24)$$